Published in "Dalton Transactions 2009: 3993-4002"
which should be cited to refer to this work.

Photochemical, photophysical and redox properties of novel fulgimide derivatives with attached 2,2′-bipyridine (bpy) and $[M(bpy)_3]^{2+}$ (M = Ru and Os) moieties

Ron T. F. Jukes,[a] Joël Kühni,[b] Nunzio Salluce,[b] Peter Belser,[b] Luisa De Cola*[c] and František Hartl*[a,d]

Fulgimides monosubstituted with $[M(bpy)_3]^{2+}$ (M = Ru, Os; bpy = 2,2′-bipyridine) chromophore units and with a single bpy group were synthesized and investigated as components of conceivable dinuclear photochromic switches of luminescence. The *E*-, *Z*- and closed-ring (C) photoisomer forms of the bpy-bound fulgimide were successfully separated by semi-preparative HPLC. The same procedure failed, however, in the case of the $[M(bpy)_3]^{2+}$-substituted fulgimides. Energy transfer from the excited photochromic unit to the metal-bpy centre competes with the fulgimide cyclization, reducing the photocyclization quantum yields by approximately one order of magnitude compared to the non-complexed fulgimide-bpy ligand ($\varphi_{EC} = 0.17$, $\varphi_{EZ} = 0.071$, $\varphi_{ZE} = 0.15$ at $\lambda_{exc} = 334$ nm). The cycloreversion of the fulgimide-bpy ligand is less efficient ($\varphi_{CE} = 0.047$ at $\lambda_{exc} = 520$ nm). The intensity of the ^{3}MLCT-based luminescence of the metal-bpy chromophore (in MeCN, $\varphi_{deaer} = 6.6 \times 10^{-2}$ and $\tau_{deaer} = 1.09$ μs for Ru; $\varphi_{deaer} = 6.7 \times 10^{-3}$ and $\tau_{deaer} = 62$ ns for Os) is not affected by the fulgimide photoconversion. These results and supporting spectro-electrochemical data reveal that the lowest triplet excited states of the photochromic fulgimide moiety in all its *E*-, *Z*- and closed-ring forms lie above the lowest ^{3}MLCT levels of the attached ruthenium and osmium chromophores. The actual components are therefore unlikely to form a triad acting as functional switch of energy transfer from $[Ru(bpy)_3]^{2+}$ to $[Os(bpy)_3]^{2+}$ through the photochromic fulgimide bridge.

Introduction

Derivatives of dimethylene succinic anhydrides known as fulgides rank among the very first photochromic compounds ever synthesized.[1,2] They were described already in 1904 by Stobbe[3] who named them after the Latin verb *fulgere* ("to glisten" or "to shine"), as they were often obtained as shiny coloured crystals.[4] Stobbe observed that certain aryl fulgides changed color when exposed to light, but with the techniques and knowledge available at the time, this phenomenon could not be satisfactorily explained. It would take until the 1960's before the coloration mechanism was correctly addressed.[5]

Fulgides can bear up to four substituents at the methylidene double bonds. They exhibit a photochromic behaviour only when at least one of these substituents is an aryl group.[1,2,6] Photoexcitation of an aryl or more sophisticated dimethylfurfuryl fulgide (Scheme 1) can trigger a cyclization reaction resulting in the formation of a coloured species.[5] Excitation, however, can also result in competing *E*/*Z*-isomerization of the fulgide at the two methylidene double bonds resulting in possible co-existence of four

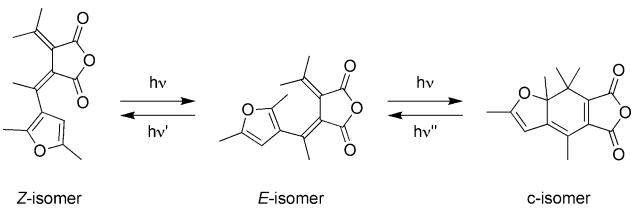

Scheme 1

geometrical isomers, *i.e.* (*E*,*E*), (*E*,*Z*), (*Z*,*E*) and (*Z*,*Z*). In most fulgides, however, one of the two methylidene carbons bears two identical substituents, usually methyl groups, so that the number of the possible *E*/*Z*-isomers is reduced to two (see Scheme 1).

Steric hindrance in the *E*- and *Z*-fulgides forces the two different cycles in the structure to twist out of plane, thereby reducing the π-conjugation in the molecule. Consequently, the electronic absorption maxima of *E*- and *Z*-fulgides are typically found in the UV region, tailing often into the visible region. Upon cyclization a new low-energy absorption band appears in the visible region. This phenomenon is explained by the extended π-conjugated system adopted by the photo-generated c-isomer where the cycles are forced by the closure of the new central ring to lie in a single plane.[7,8]

Fulgides are closely related to fulgimides that contain a succinimide group instead of the succinic anhydride.[9] Their properties and photochemical behaviour are similar. In addition, fulgimides offer the possibility to bind a substituent at the imidic nitrogen. If the latter is an electron-withdrawing group, a bathochromic shift

[a]*Van't Hoff Institute for Molecular Sciences, University of Amsterdam, Nieuwe Achtergracht 166, 1018 WV, Amsterdam, The Netherlands*
[b]*Institute of Inorganic Chemistry, University of Fribourg, Pérolles, CH-1700, Fribourg, Switzerland*
[c]*Physikalisches Institut, Westfälische Wilhelms-Universität, Mendelstrasse 7, 48149 Münster, Germany*
[d]*Department of Chemistry, The University of Reading, Whiteknights, Reading, UK, RG6 6AD. E-mail: f.hartl@reading.ac.uk; Fax: +44 118 378 6717*

of absorption maxima in electronic spectra of all the fulgimide *E*-, *Z*- and c-forms is observed.[10]

In addition to their significant potential as probes for optical data storage, photochromic compounds such as fulgimides may find more sophisticated applications in supramolecular photonic systems. One possibility is to use a photochromic moiety as a photo-addressable bridge between an energy donor and acceptor, switching the energy transfer ON and OFF by reversibly converting the bridge. In our previous work, the suitability of two other classes of photochromic compounds, *viz.* diarylethenes[11,12] and spiropyrans,[13,14] for switching energy transfer between a $[Ru(bpy)_3]^{2+}$-type donor and an $[Os(bpy)_3]^{2+}$-type acceptor was evaluated. In a true energy transfer switch, the photochromic bridge hinders energy transfer from the donor to the acceptor in the OFF state, and promotes it in the ON state. One way to achieve this goal would be to create a system where in the OFF state the energy levels of the photochromic bridge lie above those of both the donor and acceptor termini, and energy transfer, if any, takes place by means of a super-exchange mechanism, while in the ON state the levels of the bridge are in between those of the donor and acceptor, resulting in a hopping mechanism for the energy transfer (see Fig. 1).[15]

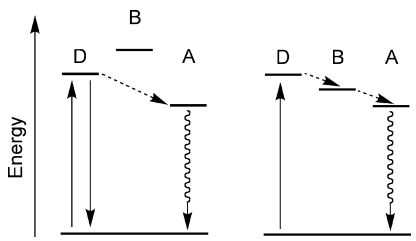

Fig. 1 Simplified energy diagrams for the proposed switchable D–B–A system. Left: long-range energy transfer occurs between the donor (D) and acceptor (A). The bridge (B) does not facilitate the process. Right: efficient energy transfer occurs between D and A through B.

This pioneering work examines the potential of fulgimides to act as photochromic bridges in such switchable triads, first of all concentrating on model mononuclear compounds (dyads). For this goal fulgimides singly substituted with 2,2′-bipyridine (bpy) and $[M(bpy)_3]^{2+}$ (M = Ru, Os) moieties were synthesized and a study of their photophysical, photochemical and redox properties was conducted.

Experimental

Reagent-grade chemicals for syntheses were obtained from Fluka, Aldrich, and Acros Chemicals and used without further purification. Solvents for syntheses were distilled from appropriate drying agents.[16] All spectroscopic experiments were carried out in spectroscopic-grade solvents purchased from Merck. For HPLC experiments, HPLC-grade acetonitrile and millipore purified water were used.

(3*E*)-1-[4-(2,2′-Bipyridine-6-yl)benzyl]-3-[1-(2,5-dimethylthien-3-yl)ethylidene]-4-(1-methylethylidene)pyrrolidine-2,5-dione (F1*E*) (see Scheme 2)

Step (a). (*Z*)-2-(1-(2,5-Dimethylthiophen-3-yl)ethylidene)-3-(propan-2-ylidene)succinic anhydride (**F2**) (0.7 g; 2.54 mmol) and 4-(4-aminophenyl)-2,2′-bipyridine (**F3**) (0.66 g; 2.53 mmol) were dissolved in dichloromethane (50 mL), and treated at 40 °C for 3 h. After solvent evaporation, the crude monoamidated product **F4** was purified by column chromatography on silica gel using CH_2Cl_2–MeOH (9 : 1) as eluent. Yield 1.22 g, 89%. ^{1}H NMR (400 MHz, $CDCl_3$): δ 1.8 (s, 3H), 1.9 (s, 3H), 2.1 (s, 3H), 2.2 (s, 3H), 2.3 (s, 3H), 4.3 (s, 2H), 5.8 (s, 1H), 6.4 (s, 1H), 7.1 (d, ^3J = 8.1 Hz, 2H), 7.3 (m, 1H), 7.5 (dd, ^3J = 3.5 Hz, 1H), 7.7 (d, ^3J = 7.6 Hz, 2H), 7.8 (m, 1H), 8.4 (d, ^3J = 8.1 Hz, 1H), 8.6 (s, 1H), 8.7 (m, 2H). ^{13}C NMR (101 MHz, $CDCl_3$): δ 13.3, 15.1, 21.8, 30.9, 44.0, 118.8, 121.3, 121.5, 123.9, 124.4, 126.2, 127.5, 128.5, 133.1, 136.6, 137.0, 137.5, 137.9, 138.3, 148.6, 149.2, 149.7, 156.0, 156.7, 171.4. MS (EI), *m*/*z*: 538.21 $[M + H]^+$.

Step (b). Monoamide **F4** (1.18 g, 2.19 mmol) was treated with acetyl chloride (10 mL) for 1 h at room temperature. The remaining solvent, as well as the resulting acetic acid, were removed under vacuum, and the residue was neutralized by a mixture of ice and saturated aqueous solution of $NaHCO_3$. The organic product was extracted with CH_2Cl_2 in a separating funnel and dried

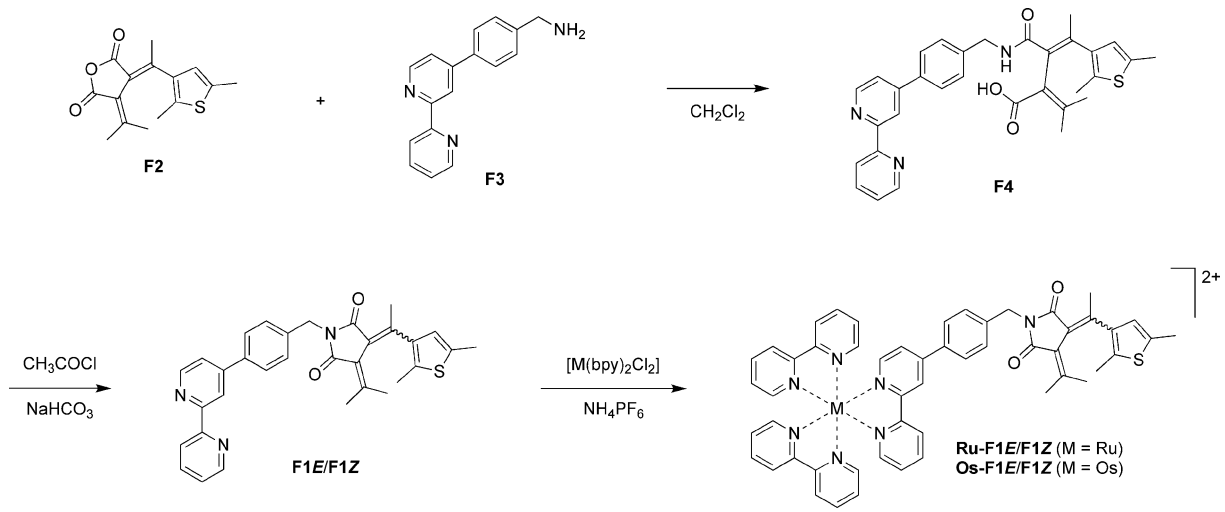

Scheme 2 Synthesis of the fulgimide ligand **F1*E*/F1*Z*** and the corresponding metal complexes **Ru-F1*E*/F1*Z*** and **Os-F1*E*/F1*Z***.

with anhydrous magnesium sulfate. After solvent evaporation, the crude product was purified by flash column chromatography on silica gel, using a mixture of ethyl acetate–methanol (9 : 1) as eluent, and a mixture of **F1*E*** and **F1*Z*** was obtained. By irradiation of the mixture of **F1*E*/F1*Z*** with 313 nm light, the sample was largely converted into closed form **F1c**. Reopening of this sample by irradiation with white light, using a 450 nm cut-off filter, yielded a sample that predominantly contained **F1*E***. Pure **F1*E*** was obtained after successful separation of **F1*Z*** by HPLC (see below). Yield 0.96 g, 84%. ^{1}H NMR (400 MHz, CD_2Cl_2): δ 1.2 (s, 3H), 2.1 (s, 3H), 2.3 (s, 3H), 2.4 (s, 3H), 2.6 (s, 3H), 4.8 (s, 2H), 6.5 (s, 1H), 7.3 (m, 2H), 7.5 (d, 1H), 7.5 (d, 2H, ^3J = 8.1 Hz), 7.6 (d, 2H, ^3J = 7.1 Hz), 7.7 (d, 2H, ^3J = 8.6 Hz), 8.5 (d, 2H, ^3J = 8.1 Hz). ^{13}C NMR (101 MHz, CD_2Cl_2): δ 15.1, 15.5, 22.0, 26.6, 27.3, 41.4, 119.2, 121.6, 122.1, 124.4, 124.6, 125.7, 127.8, 127.9, 129.5, 129.8, 134.3, 135.9, 137.8, 138.1, 138.8, 141.1, 148.9, 149.3, 149.8, 150.3, 155.4, 156.7, 157.3, 166.1, 168.7, 169.1. MS (EI), *m/z*: 520.2 [M + H]$^+$. Elemental analysis calcd (%) for $C_{32}H_{29}N_3O_2S$ (519.20): C 73.96, H 5.62, N. 8.09; found: C 73.68, H 5.70, N 7.89.

[Ru(bpy)$_2$(F1*E*/F1*Z*)](PF$_6$)$_2$ (Ru-F1*E*/F1*Z*)

In a two-necked 50 mL flask, ligand **F1*E*** (60 mg, 0.11 mmol) and $[Ru(bpy)_2Cl_2]$ (61 mg, 0.13 mmol) were suspended under argon atmosphere in deaerated ethanol (30 mL). The mixture was refluxed for 3 h. After evaporation of the ethanol, the remaining solid was redissolved in water and washed with CH_2Cl_2. Addition of NH_4PF_6 caused precipitation of the complex in the water phase. The precipitate was isolated by filtration under reduced pressure, dried in the air overnight and purified by column chromatography (SiO_2) using a mixture of MeCN–MeOH–KNO_3-solution (4 : 1 : 1; the KNO_3 solution was prepared by dissolution of 1 g of KNO_3 in 10 mL of H_2O) as eluent, to give **Ru-F1*E*/F1*Z***. Isomers **Ru-F1*E*** and **Ru-F1*Z*** were present in *ca.* 1 : 1 ratio. They could be separated by HPLC (see below) but attempts to obtain pure solids were unsuccessful. Yield 109 mg, 78%. ^{1}H NMR (300 MHz, CD_3CN): δ 1.22 (s, 3H (**Ru-F1*E***)), 1.96 (s, 3H (**Ru-F1*Z***)), 2.03 (s, 3H (**Ru-F1*Z***)), 2.09 (s, 3H (**Ru-F1*E***)), 2.22 (s, 6H (**Ru-F1*E*/F1*Z***)), 2.37 (s, 6H (**Ru-F1*E*/F1*Z***)), 2.39 (s, 3H (**Ru-F1*Z***)), 2.55 (s, 3H (**Ru-F1*E***)), 4.68 (s, 2H (**Ru-F1*Z***)), 4.80 (s, 2H (**Ru-F1*E***)), 6.56 (s, 1H (**Ru-F1*Z***)), 6.63 (s, 1H (**Ru-F1*E***)), 7.36–7.47 (m, 12H (**Ru-F1*E*/F1*Z***)), 7.51 (d, 2H, ^3J = 8.4 Hz (**Ru-F1*E***)), 7.61 (t, 2H, ^3J = 5.7 Hz (**Ru-F1*E*/F1*Z***)), 7.70–7.85 (m, 16H (**Ru-F1*E*/F1*Z***)), 8.06 (t, 10H, ^3J = 7.8 Hz (**Ru-F1*E*/F1*Z***)), 8.50 (d, 10H, ^3J = 7.8 Hz (**Ru-F1*E*/F1*Z***)), 8.65 (d, 1H, ^3J = 8.1 Hz (**Ru-F1*Z***)), 8.71 (d, 1H, ^3J = 5.4 Hz (**Ru-F1*E***)). ^{13}C NMR (101 MHz, CD_3CN): δ 14.1, 14.7, 14.9, 15.0, 25.5, 118.2, 122.8, 125.3, 125.7, 126.3, 126.8, 128.5, 128.6, 129.5, 129.7, 134.5, 135.7, 136.0, 138.1, 138.6, 138.7, 140.9, 141.3, 150.2, 152.5, 152.6, 157.9, 158.2, 168.8, 168.9, 169.3. MS (ESI), *m/z*: 1078.2 [M – PF$_6$]$^+$. Elemental analysis calcd (%) for $C_{52}H_{45}F_{12}N_7O_2P_2RuS$ (1223.17): C 51.07, H 3.71, N. 8.02; found: C 50.86, H 3.79, N 7.83.

[Os(bpy)$_2$(F1*E*/F1*Z*)](PF$_6$)$_2$ (Os-F1*E*/F1*Z*)

In a two-necked 50 mL flask, ligand **F1*E*** (60 mg, 0.11 mmol) and $[Os(bpy)_2Cl_2]$ (72 mg, 0.13 mmol) were suspended under argon atmosphere in deaerated methoxyethanol (30 mL). The mixture was refluxed for 7 h. After evaporation of the methoxyethanol, the remaining solid was redissolved in water and washed with CH_2Cl_2. Addition of NH_4PF_6 caused precipitation of the complex in the water phase. The precipitate was isolated by filtration under reduced pressure, dried in the air overnight and purified by column chromatography (SiO_2) using a mixture of MeCN–MeOH–KNO_3-solution (4 : 1 : 1; the KNO_3 solution was prepared by dissolution of 1 g of KNO_3 in 10 mL of H_2O) as eluent, to give **Os-F1*E*/F1*Z***. Isomers **Os-F1*E*** and **Os-F1*Z*** were present in *ca.* 1 : 1 ratio. They could be separated by HPLC (see below) but attempts to obtain them as pure solids were unsuccessful. Yield 59 mg, 35%. ^{1}H NMR (300 MHz, CD_3CN): δ 1.23 (s, 3H (**Os-F1*E***)), 1.97 (s, 3H (**Os-F1*Z***)), 2.03 (s, 3H (**Os-F1*Z***)), 2.09 (s, 3H (**Os-F1*E***)), 2.23 (s, 6H (**Os-F1*E*/F1*Z***)), 2.37 (s, 6H (**Os-F1*E*/F1*Z***)), 2.39 (s, 3H (**Os-F1*Z***)), 2.55 (s, 3H (**Os-F1*E***)), 4.69 (s, 2H (**Os-F1*Z***)), 4.81 (s, 2H (**Os-F1*E***)), 6.56 (s, 1H (**Os-F1*Z***)), 6.63 (s, 1H (**Os-F1*E***)), 7.27–7.34 (m, 12H (**Os-F1*E*/F1*Z***)), 7.45 (d, 2H, ^3J = 8.7 Hz (**Os-F1*E***)), 7.52 (t, 2H, ^3J = 6.3 Hz (**Os-F1*E*/F1*Z***)), 7.60–7.69 (m, 14H (**Os-F1*E*/F1*Z***)), 7.78 (d, 2H, ^3J = 8.7 Hz (**Os-F1*E***)), 7.86 (t, 10H, ^3J = 7.8 Hz (**Os-F1*E*/F1*Z***)), 8.48 (d, 10H, ^3J = 7.8 Hz (**Os-F1*E*/F1*Z***)), 8.62 (d, 1H, ^3J = 8.4 Hz (**Os-F1*Z***)), 8.68 (d, 1H, ^3J = 5.1 Hz (**Os-F1*E***)). ^{13}C NMR (101 MHz, CD_3CN) δ 118.4, 123.0, 125.5, 125.7, 126.3, 128.7, 128.8, 129.1, 129.7, 138.1, 138.2, 151.8, 151.9, 160.0. MS(ESI), *m/z*: 1168.3 [M – PF$_6$]$^+$, 511.65 [M – 2PF$_6$]$^{2+}$. Elemental analysis calcd (%) for $C_{52}H_{45}F_{12}N_7O_2OsP_2S$ (1312.23): C 47.60, H 3.46, N. 7.47; found: C 47.31, H 3.78, N 7.26.

Elemental analyses based on burning with V_2O_5 were carried out in the H. Kolbe Mikroanalytisches Laboratorium, Mülheim a.d. Ruhr, Germany.

Chromatograms for analyses were obtained on an Agilent 1100 Series HPLC with a built-in UV-vis detector, using a Varian Inertsil ODS-3 column (3 μm C_{18}, 50 × 4.6 mm). The analytical wavelength was 254 nm for both the ligands and complexes, to ensure that the separated fractions were free of substantial amounts of impurities or decomposition products.

The ligand and complex photoisomers were separated on a HP 1050 Series HPLC, coupled to a Separations UV-vis detector, using a Waters XTerra MS column (5 μm C_{18}, 100 × 19 mm). A linear solvent gradient was applied, starting with 95% H_2O/5% MeCN (containing 0.04% and 0.4% formic acid for the ligands and complexes, respectively) and changing to 95% MeCN/5% H_2O over a period of several minutes. The detection wavelength was 254 nm for the ligands. For the complexes, the detector on the semi-preparative HPLC was set to 450 nm, so that the signals for the different isomers could easily be recognized, without any interference from impurities or decomposition products.

NMR spectra were obtained on Bruker DRX-300 (300.11 MHz for ^{1}H NMR) or Bruker Avance DRX-400 (400.13 MHz for ^{1}H and 100.62 MHz for ^{13}C NMR) spectrometers. Chemical shifts (δ) are reported in ppm, using the solvent itself as internal standard. The coupling constants (J) are reported in Hz. The assignment of the NMR signals refers to the atom numbering presented in Chart 1.

UV-vis absorption spectra were recorded on Hewlett-Packard 8453 diode array or software-updated Perkin-Elmer Lambda 5 spectrophotometers, and steady-state emission spectra on a Spex 1680 spectrofluorimeter. Emission spectra were not corrected for the photomultiplier response. Deaerated solutions were prepared by the freeze-pump-thaw technique on a vacuum line. Luminescence quantum yields were determined for optically dilute

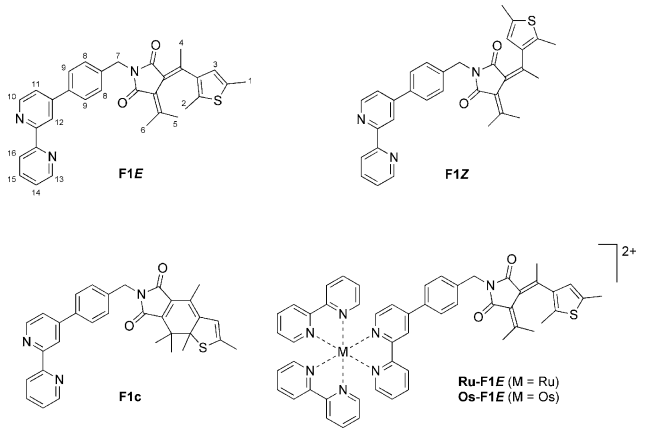

Chart 1

solutions, using solutions of $[Ru(bpy)_3]Cl_2$ in air-equilibrated H_2O ($\varphi_{em} = 0.028$)[17] or $[Os(bpy)_3](PF_6)_2$ in air-equilibrated MeCN ($\varphi_{em} = 0.0035$)[18] as references where appropriate.

Nanosecond time-resolved absorption spectra were measured using a setup described previously.[19] The irradiation source was a continuously tunable (400–700 nm) Coherent Infinity XPO laser (2 ns FWHM), operated at 10 Hz. A 50% mirror was used to divide the probe light into sample and reference beams, which greatly improved the signal-to-noise ratio.

Time-resolved emission studies in the nanosecond time domain were performed using the continuously tunable (400–700 nm) Coherent Infinity XPO laser (2 ns FWHM) as the excitation source. The emitted light was detected at a single emission wavelength, using a combination of an Oriel monochromator and a Hamamatsu P28 photomultiplier tube, from which the signal was recorded on a Tektronix TDS684B oscilloscope (1 GHz, 5 GS s^{-1}).

Photocyclization and cycloreversion quantum yields were determined by monitoring the change in the visible absorption of the photoproduct upon irradiation. To determine the quantum yields of the *E*/*Z*- and *Z*/*E*-isomerizations, HPLC responses were recorded before and after irradiation. The photoconversion was kept below 10%. A high-pressure Hg-lamp (Oriel Model 6137) in combination with appropriate interference filters served as the irradiation source. The incidental photon flux was determined before and after each measurement, using fresh toluene solutions of actinometers Aberchrome 540 ($\varphi_\lambda = 0.20$ for 313 nm $\leq \lambda \leq$ 366 nm)[20] and Aberchrome 540P ($\varphi_\lambda = 0.178–2.40 \times 10^{-4} \times \lambda$ for 440 nm $\leq \lambda \leq$ 550 nm).[21]

Cyclic voltammograms of approximately 10^{-3} M parent compounds in butyronitrile (freshly distilled from CaH_2) containing 10^{-1} M Bu_4NPF_6 electrolyte were recorded in a gastight single-compartment three-electrode cell equipped with platinum disk working (apparent surface of 0.42 mm^2), coiled platinum wire auxiliary, and silver wire pseudo reference electrodes. The cell was connected to a computer-controlled EG&G PAR Model 283 potentiostat. All redox potentials are reported against the ferrocene/ferrocenium (Fc/Fc^+) redox couple used as internal standard.[22]

UV-vis spectroelectrochemical experiments were performed in an air-tight optically transparent thin-layer electrochemical (OTTLE) cell[23] equipped with a Pt minigrid working electrode (32 wires cm^{-1}) and quartz windows. The controlled-potential electrolyses were carried out with a PA4 potentiostat (EKOM, Polná, Czech Republic).

Estimated experimental errors in the reported data are as follows. Absorption and emission maxima ± 2 nm; emission lifetimes ± 8%; emission quantum yields ± 20%; photocyclization quantum yields ± 10%, redox potentials ± 10 mV.

Table 1 ^{1}H NMR data for **F1*E***, **F1*Z*** and **F1c**[a]

Compound	δ/ppm
F1*E*	1.23 (s, 3H (5)), 2.10 (s, 3H (1)), 2.24 (s, 3H (6)), 2.37 (s, 3H (2)), 2.56 (s, 3H (4)), 4.80 (s, 2H (7)), 6.63 (s, 1H (3)), 7.41 (t, 1H (14)), 7.47 (d, 2H (8)), 7.65 (d, 1H (11)), 7.79 (d, 2H (9)), 7.91 (t, 1H (15)), 8.46 (d, 1H (16)), 8.69 (m, 3H (10, 12 and 13))
F1*Z*[b]	1.97 (s, 3H), 2.03 (s, 3H), 2.24 (s, 3H), 2.38 (s, 3H), 2.40 (s, 3H), 4.69 (s, 2H (7)), 6.57 (s, 1H (3)), 7.41 (m, 3H (8 and 14)), 7.63 (d, 1H (11)), 7.75 (d, 2H (9)), 7.90 (t, 1H (15)), 8.45 (d, 1H (16)), 8.68 (m, 3H (10, 12 and 13))
F1c[b]	1.33 (s, 3H), 1.57 (s, 3H), 1.59 (s, 3H), 2.11 (s, 3H), 2.19 (s, 3H), 4.67 (s, 2H (7)), 6.16 (s, 1H (3)), 7.43 (t, 1H (14)), 7.47 (d, 2H (8)), 7.67 (d, 1H (11), 7.81 (d, 2H (9)), 7.93 (t, 1H (15)), 8.48 (d, 1H (16)), 8.71 (m, 3H (10, 12 and 13))

[a] In CD_3CN. [b] Methyl signals could not be assigned.

Results and discussion

Separation of isomers by HPLC

Ligand **F1** was obtained predominantly in the *E*-form. It was further purified by semi-preparative HPLC, using a linear solvent gradient of MeCN and H_2O containing 0.04% formic acid. By irradiation of a solution of **F1*E***, a mixture of the *E*-, *Z*- and c-isomers was obtained. Pure samples of **F1*Z*** and **F1c** were subsequently obtained by separation over a semi-preparative HPLC column, using the same protocol.

The purity of all three isomers was confirmed by ^{1}H NMR and analytical HPLC. The ^{1}H NMR data for these isomers in CD_3CN are given in Table 1.

Complexes **Ru-F1** and **Os-F1** were synthesized from **F1*E***, but obtained as mixtures of the *E*- and *Z*-forms. The equilibration of the *E*- and *Z*-forms during the reaction is believed to be a thermal process. Attempts were made to obtain pure samples of the two isomers using semi-preparative HPLC. In the first instance, the same protocol was followed as for the separation of the different isomers of ligand **F1**. However, satisfactory separation of the *E*- and *Z*-forms of **Ru-F1** and **Os-F1** on the column was not achieved with this approach. The corresponding chromatogram showed only broad, poorly resolved peaks. This result has been ascribed to the low ionic strength of the eluent. **Ru-F1** and **Os-F1** are charged complexes and require counterions to neutralize this charge. As soon as the complexes are separated from the counterions on the HPLC column, they will stick to the column material if the ionic strength of the eluent is insufficient to compensate for the charge development. This process results in peak broadening.

In order to prove this assumption, the concentration of formic acid in the eluent was increased from 0.04% to 0.4%. As expected, the peaks in the chromatogram became significantly narrower. Analytical HPLC measurements of the eluted fractions revealed

that the *E*- and *Z*-forms of the complexes had been successfully separated.

After evaporation of the eluent, the samples of the purified isomers were redissolved in MeCN, and studied by analytical HPLC once more, to verify their purity. Unexpectedly, all samples were found to consist again of almost equimolar mixtures of the *E*- and *Z*-forms. In addition, a number of new peaks appeared in the chromatogram, which did not correspond to any of the *E*-, *Z*- or c-isomers. They were therefore assigned to decomposition products.

Initially, it was assumed that the photochemical *E*/*Z*- and *Z*/*E*-isomerization reactions for **Ru-F1** and **Os-F1** were very efficient (but not very clean), and that the purified samples had not been properly protected from stray light. However, when the experiment was repeated, keeping the solutions in the dark permanently, the result was the same. Also, when one of the pure fractions was exposed to daylight for several minutes, subsequent analysis by HPLC revealed no significant change in the sample composition.

Next, the possibility of a thermal equilibrium between the *E*- and *Z*-isomers was investigated. Fractions containing one of the two isomers in high purity were kept in the dark at room temperature for several days. Analysis by HPLC indicated that the composition of these samples remained unchanged over time. It also did not matter whether the solvent was removed at elevated temperatures in a rotary evaporator, or at room temperature by flowing nitrogen gas over the sample. In both cases the solutions had contained one predominant isomer before the eluent was evaporated, and a mixture was obtained after dissolution of the solid.

The increase in the formic acid concentration caused by the evaporation of the eluent was suspected to be the reason for both the equilibration and decomposition. Therefore, the eluent was changed to a pH-neutral mixture of MeCN and aqueous $2{\cdot}10^{-2}$ M NH_4HCO_3. Using this mixture, the retention times and peak widths of the *E*- and *Z*-forms were largely the same as for the eluent containing 0.4% formic acid. Unfortunately, the change in the eluent did not prevent the equilibration of the *E*- and *Z*-forms upon evaporation of the solvent either.

Having excluded the three possible origins of the complications, and lacking any other explanation for the equilibration, or a method to avoid it, the separation of the *E*- and *Z*-isomers of **Ru-F1** and **Os-F1** to obtain pure solids was abandoned.

Finally, samples of **Ru-F1*E*/F1*Z*** and **Os-F1*E*/F1*Z*** were irradiated with 334 nm light until the maximum amount of the c-forms was present. Separation of **Ru-F1c** and **Os-F1c** from their corresponding *E*- and *Z*-forms was then attempted, having used the eluent mixture containing $2{\cdot}10^{-2}$ M NH_4HCO_3, in a hope that the cyclized molecules would remain stable upon evaporation of the eluent. Unfortunately, the separation was not successful, as the *E*- and c-forms were found to have equal retention times on the preparative column, regardless of the solvent gradient employed.

Summarizing this part, all attempts to obtain pure samples of the different isomers of **Ru-F1** and **Os-F1** failed, and no satisfactory explanation for the equilibration between the *E*- and *Z*-forms of these complexes upon evaporation of the HPLC eluent has been found. Consequently, we decided to study the mixtures and concentrate on a qualitative description of the isomer properties.

Table 2 Absorption maxima and molar absorption coefficients of **F1*E***, **F1*Z*** and **F1c**[a]

Compound	λ_{max}/nm ($\varepsilon_{max}/10^4$ M^{-1} cm^{-1})
F1*Z*	246 (5.0), 271 (3.7), 340 (0.53)
F1*E*	246 (5.0), 271 (3.7), 330 (0.71)
F1c	244 (4.1), 271 (3.4), 330 (0.39), 521 (0.64)
Ru-F1*E*/F1*Z*[b]	246 (4.7), 289 (8.2), 360 (1.0), 456 (1.6)
Ru-F1c[c]	245 (2.9), 288 (7.4), 360 (0.59), 460 (1.9), 536 (1.1)
Os-F1*E*/F1*Z*[d]	246 (4.9), 292 (8.7), 371 (1.4), 486 (1.5), 585 (0.45)
Os-F1c[c]	246 (2.3), 290 (7.2), 372 (1.0), 492 (2.2), 558 (1.2)

[a] Conditions: MeCN solutions at 293 K. [b] Mixture of 43% **Ru-F1*E*** and 57% **Ru-F1*Z***. The UV-Vis absorption spectra of **Ru-F1*E*** and **Ru-F1*Z*** are assumed to be virtually identical. [c] Computed values. [d] Mixture of 39% **Os-F1*E*** and 61% **Os-F1*Z***. Absorption spectra of **Os-F1*E*** and **Os-F1*Z*** are assumed to be virtually identical.

Electronic absorption properties

UV-Vis absorption spectra of **F1*E***, **F1*Z*** and **F1c** in MeCN are shown in Fig. 2. Absorption maxima and the corresponding molar absorption coefficients, ε_{max}, are reported in Table 2.

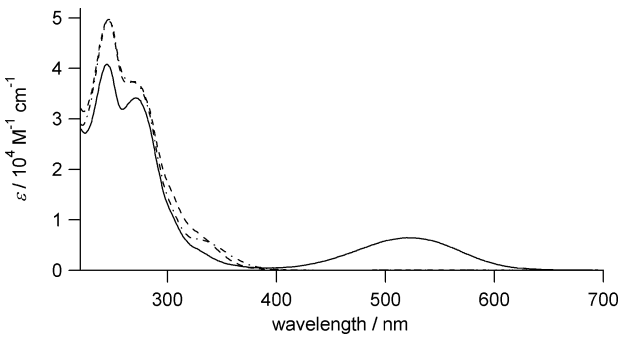

Fig. 2 UV-vis absorption spectra of **F1*E*** (---), **F1*Z*** (-·-) and **F1c** (—) in MeCN solutions at 293 K.

The electronic absorption spectra of **F1*E*** and **F1*Z*** are almost identical. The only notable difference is the shape of the weak absorption band in the 300–400 nm region. Differently from **F1*E*** and **F1*Z***, cyclized **F1c** exhibits an absorption band in the visible region, as a result of the more extended π-conjugation in this molecule.[7,8] The positions and intensities of the absorption bands of **F1*E***, **F1*Z*** and **F1c** compare well with those of similar fulgimides.[24,25]

Fig. 3 displays the electronic absorption spectrum of a mixture of **Ru-F1*E*** and **Ru-F1*Z*** in MeCN. As the differences between the absorption spectra of ligands **F1*E*** and **F1*Z*** are very small, it is therefore reasonable to assume that the spectra of **Ru-F1*E*** and **Ru-F1*Z*** are essentially identical, and that the displayed spectrum is a good representation of both. The absorption spectrum of the reference complex $[Ru(bpy)_3]^{2+}$ is also shown in Fig. 3. From the overlap of the two spectra, it is clear that there is no wavelength at which the fulgimide part of the molecule can be excited selectively. The difference between the two spectra is largest between 300–350 nm. Light from this wavelength interval was therefore used to excite the fulgimide part of the molecule.

The electronic absorption spectrum of a mixture of **Os-F1*E*** and **Os-F1*Z*** in MeCN is shown in Fig. 4. As for **Ru-F1**, we expect the absorption spectra of **Os-F1*E*** and **Os-F1*Z*** to be

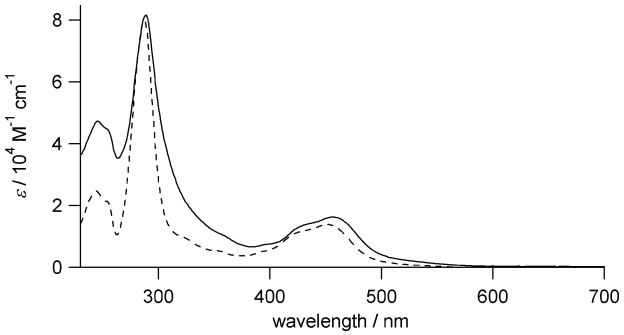

Fig. 3 UV-vis absorption spectra of a mixture of 43% **Ru-F1*E*** and 57% **Ru-F1*Z*** (—), and reference $[Ru(bpy)_3]^{2+}$ (---) in MeCN at 293 K.

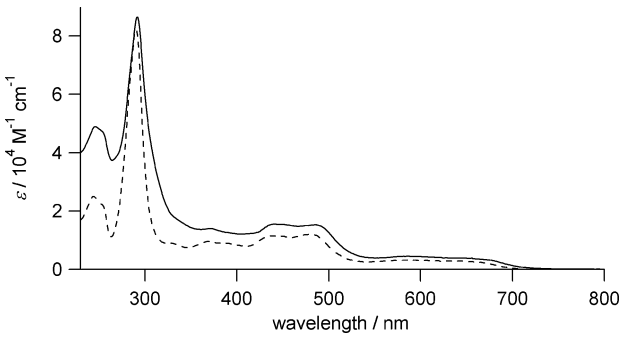

Fig. 4 UV-vis absorption spectra of a mixture of 39% **Os-F1*E*** and 61% **Os-F1*Z*** (—), and reference $[Os(bpy)_3]^{2+}$ (---) in MeCN at 293 K.

essentially identical, and the displayed spectrum is therefore a fair representation of both. Similar to **Ru-F1**, the 290–350 nm region is most suited for the electronic excitation of the fulgimide species.

Upon irradiation of the mixture of **Ru-F1*E*** and **Ru-F1*Z*** with 334 nm light, a new absorption band grows in the visible region, which is attributed to **Ru-F1c**. After several hours of irradiation, this band no longer increases in intensity, and eventually starts to diminish as a result of photodecomposition. The same behaviour was observed for the mixture of **Os-F1*E*** and **Os-F1*Z***.

We followed the photoconversion to the c-forms in CD_3CN by ^1H NMR. The relative amounts of the different isomers were determined from the intensities of the H(3)-signals. These intensities were determined relative to that of the 2,2′-bipyridine signal around 8.5 ppm. The ^1H NMR data for **F1** (see Table 1) show that the latter signal appears for all three isomers and its intensity is therefore not affected by the conversion. When decomposition of the complexes occurs, it is assumed to involve either the fulgimide moiety or the spacer between the fulgimide and the modified bpy ligand, but not the appended metal complex. Therefore, the intensity of the 2,2′-bipyridine signal at 8.5 ppm should remain constant. Using this reference, we were able to compensate for the effect of decomposition on the intensity of the H(3)-signals.

After prolonged irradiation with 334 nm light, the representation of **Ru-F1c** in the **Ru-F1** mixture eventually reached 19%, while a maximum of 20% **Os-F1c** was achieved in the **Os-F1** mixture. The conversion is clearly accompanied by a significant degradation of the complex and upon further irradiation the signals for all three isomers start to decrease, until the sample is completely destroyed.

Using the electronic absorption spectra of the mixtures containing the maximum amount of the c-form, the absorption spectra of pure **Ru-F1c** (see Fig. 5) and pure **Os-F1c** (see Fig. 6) were constructed. The intensity of the bands has some degree of uncertainty, as the error in determining the relative intensities of the H3-signals is still quite large, and the effect of the photodecomposition products observed by NMR on the absorption spectra is unknown.

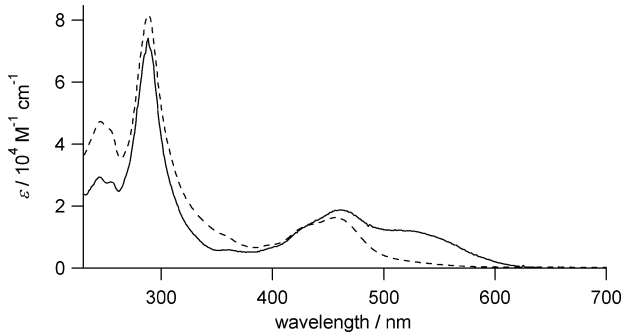

Fig. 5 UV-vis absorption spectra of **Ru-F1c** (—, computed spectrum) and of a mixture of **Ru-F1*E*** and **Ru-F1*Z*** (---) in MeCN solutions at 293 K.

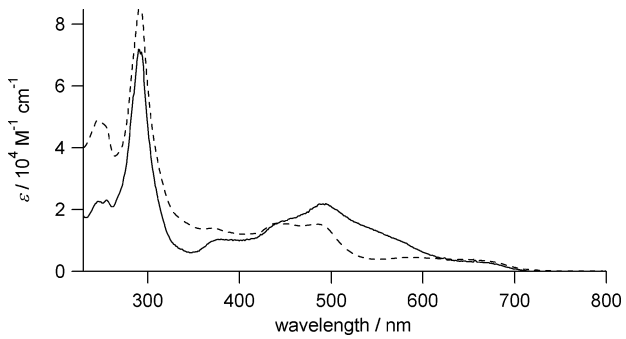

Fig. 6 UV-vis absorption spectra of **Os-F1c** (—, computed spectrum) and of a mixture of **Os-F1*E*** and **Os-F1*Z*** (---) in MeCN solutions at 293 K.

After having subtracted the absorption of the *E*/*Z*-mixtures from the computed spectra of the c-forms the new band in the visible region was found to have its absorption maximum at 524 nm for both **Ru-F1c** and **Os-F1c**. This transition is only slightly shifted compared to **F1c**, indicating that the attachment of the metal center does not significantly alter the electronic properties of the fulgimide species. The molar absorption coefficients of the new absorption bands are approximately 1.5 times higher for **Ru-F1c** and **Os-F1c** compared to **F1c**, but this may be partly due to an error in the determination of the amount of the c-form in the mixtures of the complexes.

Photoreaction quantum yields

All the investigated compounds are photoreactive. As the electronic absorption spectra of ligand isomers **F1*E*** and **F1*Z*** show very little differences, the *E*/*Z*- and *Z*/*E*-isomerizations could not be monitored by UV-vis spectroscopy. These processes were therefore followed by the analytical HPLC technique. The cyclization and cycloreversion quantum yields were determined by using UV-vis spectroscopy, as the distinct absorption of **F1c** in the visible region allows the monitoring of the cyclization reaction. Using analytical HPLC for this purpose is not advisable

Table 3 Photoisomerization quantum yields for **F1**[a]

Compound	φ_{EZ}	φ_{ZE}	φ_{EC}	φ_{CE}
F1	0.071 (334)	0.15 (334)	0.17 (334)	0.047 (520)

[a] In air-equilibrated MeCN, $T = 293$ K; λ_{exc} (nm) in brackets.

Table 4 Emission maxima (λ_{em}), quantum yields (φ_{em}), and lifetimes (τ) of **Ru-F1*E*/F1*Z*** and **Os-F1*E*/F1*Z***[a]

Compound	λ_{em}/nm	φ_{aer}	φ_{deaer}	τ_{aer}/μs	τ_{deaer}/μs
Ru-F1*E*/F1*Z*	621	1.2×10^{-2}	6.6×10^{-2}	0.18	1.09
Os-F1*E*/F1*Z*	742	4.6×10^{-3}	6.7×10^{-3}	0.042	0.062

[a] In MeCN, $T = 293$ K; $\lambda_{exc} = 450$ nm.

in this case, as the of the peaks for **F1*E*** and **F1c** overlap in the chromatogram.

The photoreaction quantum yields determined for fulgimide compound **F1** are listed in Table 3. The values compare reasonably well with those reported for fulgides and fulgimides similar to **F1**.[26–30]

As the separation of the different isomers of **Ru-F1** and **Os-F1** was unsuccessful, no attempts were made to obtain the exact photoisomerization quantum yields for these compounds. It can be concluded from irradiation experiments, however, that the cyclization quantum yields $\varphi_{EC(334)}$ for **Ru-F1*E*** and **Os-F1*E*** are reduced by approximately one order of magnitude compared to that for **1*E***. Such a decrease is attributed to depopulation of the reactive fulgimide-localized excited states by electronic energy transfer to the non-reactive metal-to-bpy charge transfer states. This claim is further corroborated by nanosecond transient absorption measurements presented herein.

Luminescence properties

Emission data for **Ru-F1** and **Os-F1** are reported in Table 4. The three isomers of ligand **F1** are non-luminescent.

The mixture of **Ru-F1*E*** and **Ru-F1*Z*** emits at $\lambda_{em} = 621$ nm in MeCN, and that of **Os-F1*E*** and **Os-F1*Z*** at $\lambda_{em} = 742$ nm (see Fig. 7). The positions, shapes and intensities of the emission bands, as well as the emission lifetimes (see Table 4) point to their origin in the Ru-to-bpy ^{3}MLCT[31] and Os-to-bpy ^{3}MLCT[32] excited states, respectively. As the emission arises from the $[M(bpy)_3]^{2+}$ chromophore, and the electronic properties of the fulgimide *E*- and *Z*-forms are very similar, the luminescence of the *E*- and *Z*-isomers should be essentially identical. The mono-exponential decays found for the emission of the mixtures (see Table 4) support this assumption.

An emission spectrum was also recorded for the mixture of the three isomers of **Ru-F1** containing the maximum amount of **Ru-F1c** (19%). The photoconversion to the c-form does not affect the emission quantum yield or lifetime of the mixture. The same applies for the mixture of the three isomers of **Os-F1** containing the maximum amount of **Os-F1c** (20%).

Evidently, neither the ruthenium-bpy, nor the osmium-bpy ^{3}MLCT emission is quenched by the fulgimide in its closed form. The lowest ^{3}IL levels of the closed fulgimide will therefore lie above the ^{3}MLCT levels of both the osmium and ruthenium bipyridine moieties. From these observations, it can be concluded that connecting a $[Ru(bpy)_3]^{2+}$-type donor and an $[Os(bpy)_3]^{2+}$-type acceptor by a photochromic bridge based upon the type of fulgimide employed in this study, will most likely not yield the desired dinuclear energy transfer switch depicted in Fig. 1, as the fulgimide will not promote energy transfer between the donor and acceptor termini by a hopping mechanism in any of its isomer forms.[33]

Time-resolved transient absorption spectroscopy

For ligand **F1**, transient absorption spectra were recorded for mixtures of the three isomers. The reason for this necessary choice is that the very weak transient observed requires accumulation of a large number of frames to obtain a well-resolved spectrum. The amount of light absorbed during this process will unavoidably convert any of the pure isomers to a mixture, and the material was not available in a sufficient amount to perform a flow-cell experiment.

Laser excitation of a mixture of **F1*E***, **F1*Z*** and **F1c** with 300 nm light resulted in a weak transient consisting of two absorption bands with maxima around 390 and 540 nm (see Fig. 8). This excited state species has a lifetime somewhere between 300–500 ns under deaerated and 100–200 ns under air-equilibrated conditions. Because of the low intensity of the transient absorption, the excited state lifetime was not determined with higher accuracy. When a single frame had been recorded directly after excitation, the same transient species was observed for both pure **F1*E*** and **F1*Z***. Upon excitation with 520 nm light, thereby having selectively excited **F1c**, no transient species was observed. The transient has therefore

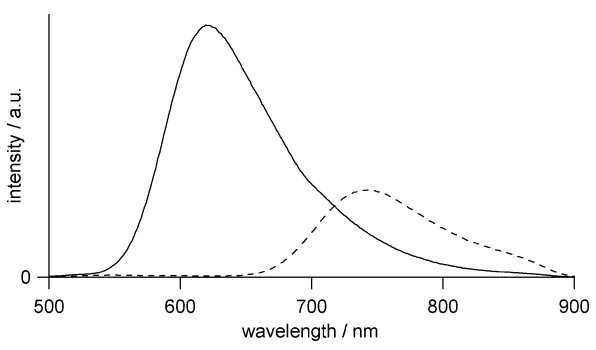

Fig. 7 Emission spectra of **Ru-F1*E*/F1*Z*** (—) and **Os-F1*E*/F1*Z*** (---) recorded in air-equilibrated MeCN at 293 K, using $\lambda_{exc} = 450$ nm.

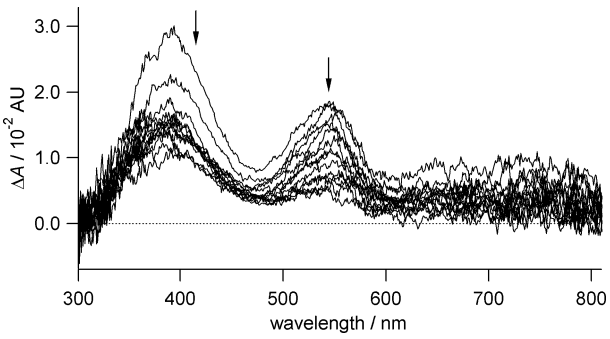

Fig. 8 Transient absorption difference spectrum of a mixture of **F1*E***, **F1*Z*** and **F1c** in deoxygenated MeCN at 293 K, with a step size of 40 ns between frames. Excitation wavelength $\lambda_{exc} = 300$ nm.

been assigned tentatively to the triplet states of both **F1*E*** and **F1*Z***. These states do not necessarily have the same lifetimes, which may partly explain the rather poor fits for the decay traces.

Fig. 9 shows the transient absorption spectrum of **Ru-F1*E*/F1*Z***. The shape of the spectrum does not depend on whether the sample was excited with 300 or 450 nm light. The recorded pattern is characteristic of a ruthenium-to-bpy ^{3}MLCT excited state.[34] The excited-state species decays back to the ground state mono-exponentially, with lifetimes of 180 and 930 ns in the presence and absence of oxygen, respectively. These values agree reasonably well with the emission lifetimes, supporting again the ^{3}MLCT nature of the luminescence. The spectral shape of the transient absorption spectrum does not change during the decay.

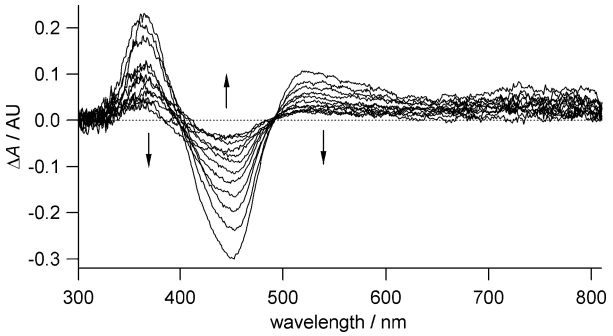

Fig. 9 Transient absorption difference spectrum of **Ru-F1*E*/F1*Z*** in deaerated MeCN at 293 K, with a step size of 100 ns between frames. Excitation wavelength $\lambda_{exc} = 450$ nm.

For **Os-F1*E*/F1*Z***, a nanosecond transient absorption spectrum is observed that can be assigned[35] to an osmium-to-bpy ^{3}MLCT excited state (see Fig. 10). As was the case for **Ru-F1*E*/F1*Z***, the transient absorption spectra obtained upon excitation with 300 or 450 nm light are identical. Excited-state lifetimes of 39 and 71 ns are found for solution of **Os-F1*E*/F1*Z*** in air-equilibrated and deoxygenated MeCN, respectively. Also in this case, these values are in good agreement with the lifetimes obtained from the emission decay measurements.

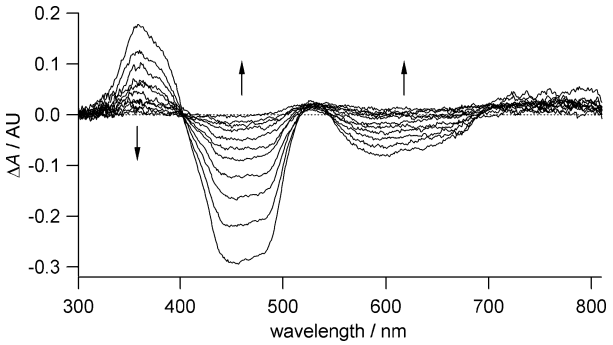

Fig. 10 Transient absorption difference spectrum of **Os-F1*E*/F1*Z*** in deaerated MeCN at 293 K, with a step size of 8 ns between frames. Excitation wavelength $\lambda_{exc} = 450$ nm.

For both **Ru-F1*E*/F1*Z*** and **Os-F1*E*/F1*Z***, only the ^{3}MLCT excited states are observed, independent of the excitation wavelength. The shapes of the spectra do not change with time and the transient species assigned to the excited triplet state of fulgimide **F1*E*/F1*Z*** is not observed in either case, despite the fact that at 300 nm a significant part of the excitation energy is absorbed directly by the fulgimide species. Evidently, energy is transferred from the fulgimide-centred excited states to the ^{3}MLCT levels on a sub-nanosecond timescale, for both **Ru-F1*E*/F1*Z*** and **Os-F1*E*/F1*Z***. The ^{3}MLCT levels of both $Ru(bpy)_3$ and $Os(bpy)_3$ chromophores thus lie at lower energies than the excited triplet states of the open fulgimide.

It has been shown that the cyclization reactions of **Ru-F1*E*/F1*Z*** and **Os-F1*E*/F1*Z*** are quenched as a result of energy transfer from the fulgimide to the metal center, but how the energy transfer takes place still has to be explained. The photochemical conversions of fulgides are primarily singlet excited-state processes.[1,2,36,37] Picosecond time-resolved absorption studies of fulgides have shown that cyclization from the singlet excited state occurs with a time constant of several tens of picoseconds at most.[38,39] In order to achieve quenching of the cyclization reaction by a factor 10, as observed here, the energy transfer should occur with a rate constant $k_{ET} \sim 10^{11}$ s^{-1}. Such high values have been obtained only for triads containing strongly conjugated spacers.[40–45] They are unlikely for a system where the linker between the energy donor and acceptor is non-conjugated.

There are several plausible explanations of this apparent discrepancy. The simplest one assumes that the value of the rate constant for the cyclization reaction of **F1*E*** is significantly lower than those for the fulgides reported in the literature.[38,39] A much slower energy transfer process then suffices to reduce the photocyclization quantum yield ten times.

Another possible reason is the presence of the heavy metal atom in **Ru-F1*E*** and **Os-F1*E***, which promotes intersystem crossing (ISC) in these molecules from the singlet to triplet excited states localized on the fulgimide moiety. Typically, no cyclization occurs from the triplet state of fulgides.[36,37] Therefore, the ISC process may account for (a part of) the reduction of the cyclization quantum yield.

Alternatively, considering again the ISC process, the cyclization of photoexcited **F1*E*** *does* occur partly from a triplet state. Fan *et al.* have observed ISC for specific types of fulgides; in these cases cyclization takes place from both the singlet and triplet states.[46–49] In general, triplet states live much longer than the corresponding singlet states (and, indeed, we have got evidence for a long-lived triplet state of **F1*E*** from the transient absorption study). The longer triplet lifetime allows the energy transfer process to compete with the reaction, thereby reducing the cyclization quantum yield.

In order to distinguish between these alternatives, fs–ps transient absorption, triplet sensitization and triplet quenching techniques will be employed in an ongoing study of the investigated compounds and purpose-modified derivatives.

Spectro-electrochemistry

The cyclic voltammogram of the prevailing open-ring isomer **F1*E*** in butyronitrile at room temperature shows an irreversible cathodic wave at $E_{p,c} = -2.36$ V *vs.* Fc/Fc^+ ($v = 100$ mV s^{-1}). No oxidation was observed down to +1.3 V. This result corresponds with the absorption of **F1*E*** above 350 nm (Fig. 2). After *in situ* irradiation of the electrolyte with UV light of a mercury lamp, the coloured ring-closed photoproduct **F1c** becomes reduced reversibly at $E_{p,c} = -1.64$ V while its oxidation at $E_{p,a.} = +0.58$ V is an irreversible process. The experimental HOMO–LUMO energy gap of *ca.*

2.2 eV (17 700 cm^{-1}; λ_{max} = 565 nm) is in good agreement with the low-energy absorption of **F1c** at 521 nm (Fig. 2).

Complexes **Ru-F1*E*** and **Ru-F1*Z*** (in about 1 : 1 ratio, see Experimental and Table 2) in butyronitrile were initially investigated by cyclic voltammetry. The cathodic response of the isomers at room temperature and v = 100 mV s^{-1} shows a single set of three fully reversible waves at $E_{1/2}$ = −1.71, −1.92 and −2.21 V. As expected, these cathodic potentials are almost identical to those of $[Ru(bpy)_3]^{2+}$, corresponding to a bpy-localized reduction sequence.[50] Oxidation of **Ru-F1*E*/Ru-F1*Z*** is also observed as a single anodic wave at $E_{p,a}$ = +0.89 V. Differently from the reference complex, the oxidation is irreversible and cooling of the electrolyte down to 208 K is needed to observe a fully reversible one-electron Ru(II)/Ru(III) wave at $E_{1/2}$ = +0.82 V. The reduction potentials shifted slightly at this temperature to $E_{1/2}$ = −1.75, −1.92 and −2.16 V.

Unfortunately, the low yield (< 20%) of the photochemical conversion of the parent isomeric forms to **Ru-F1c** and the concomitant photodegradation prevented us to record a well-resolved cyclic voltammogram of the photoproduct.

The cyclic voltammogram of the **Ru-F1*E*/Ru-F1*Z*** mixture recorded at room temperature in a thin-layer spectroelectrochemical cell (TL-CV at v = 2 mV s^{-1}) revealed that the first bpy-localized reduction at −1.71 V became irreversible. During this cathodic step, the composed visible MLCT absorption band of the parent species at 461 nm broadened, lost intensity and shifted down to *ca.* 520 nm. The characteristic absorption of the reduced $[bpy]^{\bullet-}$ ligands (a bifurcated absorption band at *ca.* 540 nm and a broad band below 800 nm) was only rising during the fully reversible second cathodic steps at −1.92 V. This behaviour agrees with the localization of the first cathodic step at the bpy ligand attached to the fulgimide moiety. The irreversible nature of the reduction then points to some bpy-fulgimide electronic communication resulting in a secondary chemical transformation that was, however, not investigated in more detail. A similar communication can be expected also in the lowest MLCT excited state of the open-fulgimide isomers, possibly giving rise to the observed photodegradation (see above).

The Ru(II)-based oxidation and bpy-based reduction potentials of **Ru-F1*E*/Ru-F1*Z*** probably remain unaffected by the photocyclization of the fulgimide moiety. This presumption gets support from the nearly identical positions of the visible Ru-to-bpy ^{1}MLCT absorption bands in the electronic absorption spectra of **Ru-F1*E*/Ru-F1*Z*** and **Ru-F1c** (see Fig. 5). The energy difference of 2.2 eV between the frontier orbitals of the **F1c** moiety (see above) probably also does not change when attached to bpy in **Ru-F1c**. This means that, neglecting any contribution from electronic reorganization, the energy of the lowest ^{1}MLCT state of the $Ru(bpy)_3^{2+}$ centre (2.57 eV) is higher than that of the lowest ^{1}IL state of the closed fulgimide moiety. However, this does not hold obviously for the corresponding triplet excited states and the phosphorescent ^{3}MLCT level lies at the lowest energy both in **Ru-F1*E*/Ru-F1*Z*** and **Ru-F1c** (see above). A cautious comparison with related complexes bearing a photochromic spiropyran moiety,[14] indicates that a feasible photochromic energy transfer switch complying with the orbital energy diagram depicted in Fig. 1 would require the HOMO–LUMO gap in a closed-ring fulgimide to be some 0.3 eV smaller than encountered for **F1c**. A better option is to tune the properties of the energy donor moiety and raise sufficiently the energy of its lowest ^{3}MLCT state.

Conclusions

The photophysical and photochemical properties of fulgimides substituted with luminescent $[Ru(bpy)_3]^{2+}$ and $[Os(bpy)_3]^{2+}$ moieties were studied, and the results compared with those obtained for the corresponding fulgimide substituted with a non-coordinated bipyridine moiety.

The three isomers of the free ligand **F1** were separated by semi-preparative HPLC. Attempts to achieve the same kind of separation for corresponding the metal complexes failed, as a result of a peculiar equilibration process taking place upon evaporation of the eluent.

In the *E*- and *Z*-forms of the complexes, energy is transferred from the singlet or triplet fulgimide-localized excited states to the ^{3}MLCT levels localized at the metal-tris(bipyridine) chromophore. This process results in significant reduction of the efficiency of the photocyclization reaction.

The ^{3}MLCT levels of the $[Ru(bpy)_3]^{2+}$ and $[Os(bpy)_3]^{2+}$ chromophores are below the triplet energy levels of the fulgimide species, regardless of whether it is in the *E*-, *Z*- or c-form. Hence, the fulgimide will not facilitate energy transfer between these ruthenium donor and osmium acceptor termini by a hopping mechanism in any of its forms, which is a requirement for creating a true Ru-bridge-Os energy transfer switch (Fig. 1). It would nevertheless be interesting to synthesize a Ru-**F1**-Os triad in order to investigate how much the Ru-to-Os superexchange energy transfer rate becomes affected by the increased conjugation in the cyclized fulgimide compared to its open-ring form.

References

1 J. Whittall, in *Photochromism, Molecules and Systems*, ed. H. Dürr, H. Bouas-Laurent, Elsevier, Amsterdam, 1990.
2 Y. Yokoyama, *Chem. Rev.*, 2000, **100**, 1717–1739.
3 H. Stobbe, *Ber. Dtsch. Chem. Ges.*, 1904, **37**, 2236–2240.
4 H. Stobbe, *Ber. Dtsch. Chem. Ges.*, 1905, **38**, 3672–3682.
5 A. Santiago and R. S. Becker, *J. Am. Chem. Soc.*, 1968, **90**, 3654–3658.
6 H. Stobbe, *Liebigs Ann. Chem.*, 1908, **359**, 1–48.
7 L. H. Yu, Y. F. Ming, W. L. Zhao and M. G. Fan, *J. Photochem. Photobiol., A*, 1992, **68**, 309–317.
8 Y. Yoshioka and M. Irie, *Electron. J. Theor. Chem.*, 1996, **1**, 183–190.
9 R. J. Hart, H. G. Heller and K. Salisbury, *J. Chem. Soc., Chem. Commun.*, 1968, 1627–1628.
10 M. A. Wolak, C. J. Thomas, N. B. Gillespie, R. R. Birge and W. J. Lees, *J. Org. Chem.*, 2003, **68**, 319–326.
11 R. T. F. Jukes, V. Adamo, F. Hartl, P. Belser and L. De Cola, *Inorg. Chem.*, 2004, **43**, 2779–2792.
12 R. T. F. Jukes, V. Adamo, F. Hartl, P. Belser and L. De Cola, *Coord. Chem. Rev.*, 2005, **249**, 1327–1335.
13 R. T. Jukes, B. Bozic, F. Hartl, P. Belser and L. De Cola, *Inorg. Chem.*, 2006, **45**, 8326–8341.
14 R. T. F. Jukes, B. Bozic, P. Belser, L. De Cola and F. Hartl, *Inorg. Chem.*, 2009, **48**, 1711–1721.
15 J. Jortner and M. Bixon, *Electron Transfer—From Isolated Molecules to Biomolecules, Part One*, John Wiley & Sons, New York, 1999, vol. 106.
16 D. D. Perrin and W. L. F. Armarego, *Purification of Laboratory Compounds*, 3rd edn, Pergamon, Exeter, UK, 1988.
17 K. Nakamaru, *Bull. Chem. Soc. Jpn.*, 1982, **55**, 2697–2705.
18 M. Frank, M. Nieger, F. Vögtle, P. Belser, A. von Zelewsky, L. De Cola, V. Balzani, F. Barigelletti and L. Flamigni, *Inorg. Chim. Acta*, 1996, **242**, 281–291.
19 C. J. Kleverlaan, D. J. Stufkens, I. P. Clark, M. W. George, J. J. Turner, D. M. Martino, H. van Willigen and A. Vlček, Jr., *J. Am. Chem. Soc.*, 1998, **120**, 10871–10879.
20 H. G. Heller and J. R. Langan, *J. Chem. Soc., Perkin Trans. 2*, 1981, 341–343.

21 (*a*) A. P. Glaze, H. G. Heller, C. J. Morgan, S. N. Oliver and J. Whittall, in *Xth IUPAC Symposium on Photochemistry*, Interlaken, Switzerland, 1984, p. 369; (*b*) H. J. Kuhn, R. Braslavsky and R. Schmidt, *Pure Appl. Chem.*, 2004, **76**, 2105–2146.
22 G. Gritzner and J. Kůta, *Pure Appl. Chem.*, 1984, **56**, 461–466.
23 M. Krejčík, M. Daněk and F. Hartl, *J. Electroanal. Chem. Interf. Electrochem.*, 1991, **317**, 179–187.
24 R. Matsushima and H. Sakaguchi, *J. Photochem. Photobiol., A*, 1997, **108**, 239–245.
25 B. Otto and K. Ruck-Braun, *Eur. J. Org. Chem.*, 2003, 2409–2417.
26 P. J. Darcy, H. G. Heller, P. J. Strydom and J. Whittall, *J. Chem., Soc., Perkin Trans. 1*, 1981, 202–205.
27 V. Deblauwe and G. Smets, *Macromol. Chem.*, 1988, **189**, 2503–2512.
28 Y. Yokoyama, H. Hayata, H. Ito and Y. Kurita, *Bull. Chem. Soc. Jpn.*, 1990, **63**, 1607–1610.
29 A. Tomoda, A. Kaneko, H. Tsuboi and R. Matsushima, *Bull. Chem. Soc. Jpn.*, 1993, **66**, 330–333.
30 Y. C. Liang, A. S. Dvornikov and P. M. Rentzepis, *J. Mater. Chem.*, 2000, **10**, 2477–2482.
31 A. Juris, V. Balzani, F. Barigelletti, S. Campagna, P. Belser and A. von Zelewsky, *Coord. Chem. Rev.*, 1988, **84**, 85–277.
32 E. M. Kober, J. V. Caspar, R. S. Lumpkin and T. J. Meyer, *J. Phys. Chem.*, 1986, **90**, 3722–3734.
33 This conclusion is based upon the emission of dyad samples containing only ±20% of the closed fulgimide form, however. It would be prudent to verify this claim using a sample of the pure c-form, should this be obtained.
34 K. Miedlar and P. K. Das, *J. Am. Chem. Soc.*, 1982, **104**, 7462–7469.
35 C. Creutz, M. Chou, T. L. Netzel, M. Okumura and N. Sutin, *J. Am. Chem. Soc.*, 1980, **102**, 1309–1318.
36 H. D. Ilge, H. Langbein, M. Reichenbächer and R. Paetzold, *J. Prakt. Chem.*, 1981, **323**, 367–380.
37 H. D. Ilge and R. Paetzold, *J. Prakt. Chem.*, 1984, **326**, 705–720.
38 H. D. Ilge, J. Sühnel, D. Khechinashvili and M. Kaschke, *J. Photochem.*, 1987, **38**, 189–203.
39 M. Handschuh, M. Seibold, H. Port and H. C. Wolf, *J. Phys. Chem. A*, 1997, **101**, 502–506.
40 F. Barigelletti, L. Flamigni, V. Balzani, J. P. Collin, J. P. Sauvage, A. Sour, E. C. Constable and A. Thompson, *J. Chem. Soc., Chem. Commun.*, 1993, 942–944.
41 F. Barigelletti, L. Flamigni, V. Balzani, J. P. Collin, J. P. Sauvage, A. Sour, E. C. Constable and A. Thompson, *J. Am. Chem. Soc.*, 1994, **116**, 7692–7699.
42 V. Grosshenny, A. Harriman, M. Hissler and R. Ziessel, *J. Chem. Soc., Faraday Trans.*, 1996, **92**, 2223–2238.
43 A. Harriman, F. M. Romero, R. Ziessel and A. C. Benniston, *J. Phys. Chem. A*, 1999, **103**, 5399–5408.
44 A. El-Ghayoury, A. Harriman, A. Khatyr and R. Ziessel, *Angew. Chem., Int. Ed.*, 2000, **39**, 185–189.
45 A. Harriman, M. Hissler, A. Khatyr and R. Ziessel, *Eur. J. Inorg. Chem.*, 2003, 955–959.
46 W. L. Zhao, Y. F. Ming, Z. Q. Zhu and M. G. Fan, *J. Photochem. Photobiol., A*, 1992, **63**, 235–240.
47 L. Yu, Y. Ming and M. Fan, *Res. Chem. Intermed.*, 1993, **19**, 829–838.
48 L. H. Yu, Y. F. Ming, X. Y. Zhang, M. G. Fan, N. Y. Lin and S. Yao, *J. Photochem. Photobiol., A*, 1993, **74**, 37–41.
49 L. H. Yu, Y. F. Ming, W. L. Zhao and M. G. Fan, *Mol. Cryst. Liquid Cryst.*, 1994, **246**, 49–58.
50 N. Sutin and C. Creutz, *Adv. Chem. Ser.*, 1978, **168**, 1–27.